Desalination and Water Treatment
www.deswater.com

doi: 10.5004/dwt.2020.25266

191 (2020) 21–28
July

A novel integrated module for hybridization of forward osmosis (FO) and membrane distillation (MD): effect of operating conditions

Juyoung Lee, Jihyeok Choi, Yongjun Choi, Sangho Lee*

School of Civil and Environmental Engineering, Kookmin University, Jeongneung-Dong, Seongbuk-Gu, Seoul, 136-702, Korea, Tel. +82-2-910-4529; Fax: +82-2-910-4939; emails: sanghlee@kookmin.ac.kr cjh6563@gmail.com (J. Choi), cchoiyj1041@gmail.com. (Y. Choi)

Received 23 August 2019; Accepted 29 November 2019

ABSTRACT

Recently, a hybrid system consisting of forward osmosis (FO) and membrane distillation (MD) has come into the spotlight. In the FO-MD hybrid system, freshwater is obtained from feed water through the FO process and the diluted draw solution from the FO process is re-concentrated by the MD process. However, relatively little information is available on the optimization of the hybrid system of FO and MD and their combination in a single module. Accordingly, this study focused on the development of an integrated module for the FO-MD hybrid system. The module was designed, fabricated, and tested in a bench-scale system. The effect of design and operating parameters, including flow velocity, the temperature of solutions, and membrane areas, on the overall performance of the module and system, was investigated. With the control of the temperature of the draw solution, the integrated FO-MD module enabled the constant flux operation, which is essential for the practical implementation of FO technology.

Keywords: Forward osmosis (FO); Membrane distillation (MD); Integrated module; Hybridization; Operating conditions

1. Introduction

Water scarcity is being globalized due to the huge amount of increase in water demands and the great development of various kinds of industries [1]. Rapid climate change and industrialization make the challenge of presenting proper and clean drinking water more difficult and complicate [2]. In order to mitigate such issues, various desalination technologies have been developed in the past few decades [3–6]. However, commercial technologies such as reverse osmosis (RO) use a lot of energy for converting saline water to freshwater [7]. Moreover, RO has a limited recovery of 75%–85% due to its own characteristics and it means that 15%–25% of high salinity brine has to be disposed of [3,8,9]. In fact, the negative impacts of brine disposal on our ecosystem has been declared in various literature and researches [10,11]. Therefore, innovative approaches are necessary to take both indispensable objectives of the constant water resource and protection of the ecosystem [4,11–13].

In this context, forward osmosis (FO) has drawn attention as one of the innovative technologies for the desalination of seawater, brackish water, and wastewater to create an ongoing supply of freshwater [14]. FO is an osmotically-driven membrane separation that uses high osmotic pressure of draw solution as its driving force [15]. FO has many advantages such as low operation pressure and high resistance against membrane fouling [16]. These have sparked a great deal of interest from academia and industry over the past decade [14,15,17–19]. Novel membranes have been developed to revolutionize the performance of the FO process [19,20]. Mechanisms on internal concentration polarization

* Corresponding author.

Presented at the 12th International Desalination Workshop (IDW2019), 28–30 August 2019, Jeju, Korea

1944-3994/1944-3986

(ICP) and fouling have been extensively investigated together with a substantial advances in process modeling and optimization [17]. Application of FO technology has been explored for seawater desalination, wastewater reclamation, produced water treatment, and fertigation [18,21–23]. Several FO pilot plants have been also constructed and operated [24,25].

Nevertheless, the widespread use of FO technology is still limited by step for regeneration of its draw solution [19,26]. As the draw solution is diluted after the FO process, it should be concentrated again to enable its continuous use [27]. In fact, draw solution regeneration is the most energy-consuming step in FO processes because it is necessary to compensate for the mixing energy used by FO [26]. A few works have addressed the issues on the draw solution regeneration by developing novel draw solute materials and applying techniques such as reverse osmosis, nanofiltration, electrodialysis, magnetic separation, and distillation [17,18,26–29].

Among them, an emerging approach that holds potential is membrane distillation (MD) [30–32]. As one of the thermal separation processes, MD uses heat as its driving force to create the difference in the vapor pressure between the feed and the distillate sides [33]. Unlike conventional distillation technologies such as multi-stage flash and multi-effect distillation, the operation temperature of MD is relatively low (–60°C), allowing the utilization of renewable or waste heat sources [34]. This can make MD to be an economically feasible [35,36]. Moreover, the use of MD is not limited by the osmotic pressure of the feed solution, allowing MD to concentrate solutions of high osmotic pressure [37]. Accordingly, MD is suitable to regenerate a dilute draw solution [30]. In addition, FO can work as a pre-treatment process to separate multivalent/divalent ions and organic matter as well as to reduce inorganic scaling and organic fouling in the MD process [30,38]. A handful of studies have been performed to apply MD to draw solution regeneration in FO [30,38–40].

In this study, we considered the combination of FO with MD for continuous regeneration of draw solution in a novel platform. Unlike previous works on the FO-MD hybrid system in the literature, there are two main differences in our study. First, hollow fiber MD membranes were used for the hybrid system. Since hollow-fiber MD membranes exhibit large surface area per unit volume (e.g. the packing capacity of the hollow-fiber membrane module may reach 500–9,000 m^2/m^3) and high productivity per module [31], they were selected in our study. Previous researches of FO-MD hybrid system mostly focused on the use of flat sheet MD membranes for the FO process [30,40]. Second, an integrated the FO-MD module was designed and fabricated instead of combining two separate processes. Accordingly, the feed water is first treated by the FO membrane and the diluted draw solution was re-concentrated by the MD membrane in the same device. This is expected to allow a reduction in the footprint of the device and stable operation of the process.

Nevertheless, little information is available on this novel system even if there is a great deal of potential. Accordingly, the focus of this study is the investigation of the effect of operating conditions on this integrated FO-MD system under non-fouling conditions as the first step toward its practical implementation. The control of FO flux by regulating the temperature of the draw solution, which is also the feed solution to the MD, was also attempted.

2. Materials and methods

2.1. Preparation of feed and draw solutions

Deionized (DI) water was used for the feed solution (FS) of forward osmosis (FO) process and permeated solution (PS) of direct contact membrane distillation (DCMD). The draw solution, which was also used as the feed solution for MD, was prepared by dissolving a special grade NaCl (Samchun Pure Chemical Co., Ltd, Korea) into DI water and its concentration was 1.0 M.

2.2. Membranes

Flat sheet FO membranes (TORAY chemical, Inc., Seoul, Korea) were used for FO experiments. Hollow fiber PVDF membranes (Econity, Korea), which have a nominal pore size of 0.22 μm, were used for MD experiments. The characteristics of the FO and MD membranes are described in Table 1. Before the experiments, the flat sheet FO membranes were stored in DI water at 4°C after being cut and rinsed with DI water. The hollow fiber MD membranes were stored under vacuum.

2.3. Experimental setup

Two kinds of FO-MD hybrid systems were prepared for the bench-scale experiment. Fig. 1a shows the schematic diagram of the system using the integrated FO-MD module. On the other hand, Fig. 1b presents the schematic diagram of the system using separate FO and MD modules. Details on the structure of the integrated FO-MD module is illustrated in Fig. 2. The membrane area of the flat sheet FO membrane was 12 cm^2. Two bundles of the hollow fiber MD membranes were used with the total membrane area of 77.84 cm^2. The feed water was supplied through the pipe attached to the top pieces. The permeate passes through the FO membrane and is mixed with the draw solution, which is also the feed solution for the MD membrane. Eventually, the permeate is collected through the MD membrane and mixed into the distillate solution that passes inside the fibers. The flow rates were measured using flow meters. The electric conductivities of the feed and draw solutions were monitored using conductivity meters. Two water baths were used to control the temperatures of the solutions. The mass of the solution was periodically monitored by digital scales and recorded by computers to calculate flux. The FO-MD system using the separate FO and MD modules was operated under similar conditions to the system with the integrated module

2.4. Experimental procedures

A set of experiments were performed using the integrated FO-MD module (Fig. 1a) and the FO-MD hybrid system with separate modules (Fig. 1b). In each experiment,

Table 1
Membrane characteristics

FO (flat sheet)	Material	*A* (L/m² h bar)	*B* (L/m² h)	*S* (mm)
	Polyamide	6.68	0.54	0.378
DCMD (hollow-fiber)	Material	Pore size (μm)	Porosity	Tortuosity
	PVDF	0.22	0.75	2

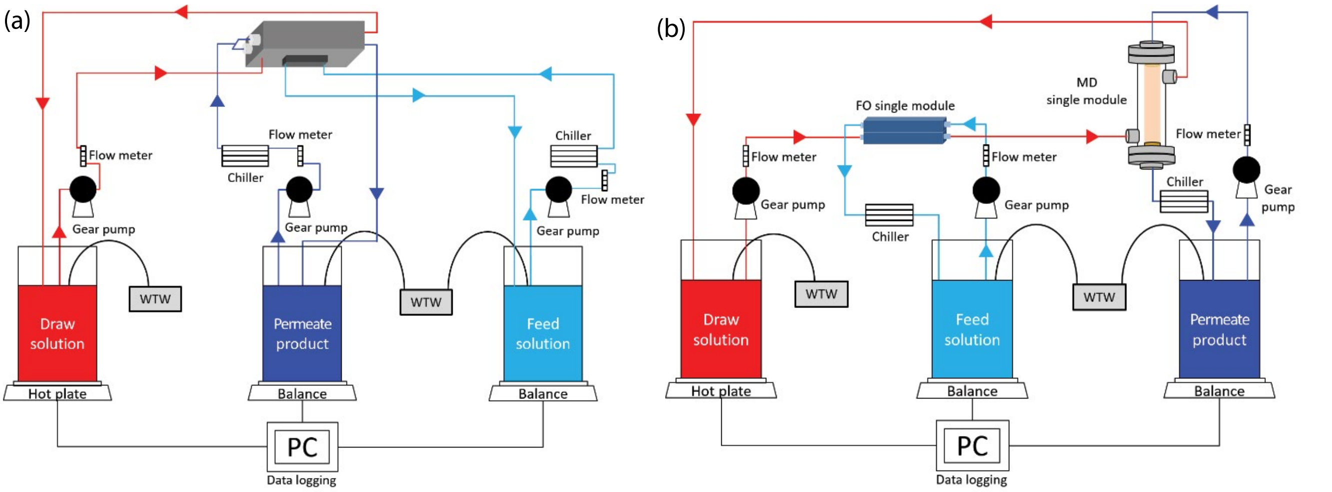

Fig. 1. Schematic diagrams of each system. (a) Integrated module system and (b) single module hybrid system.

the initial volume of the solutions was set to 2 L. The FO experiments were performed in the active layer facing on the feed solution (AL-FS) mode. The temperature of the feed solution for the FO tests was fixed at 20(±1)°C and the draw solution temperature was adjusted to 40(±1)°C, 50(±1)°C, and 60(±1)°C. The temperature of the draw solution changed since this is also the temperature for MD feed, which should be considered in the integrated module. The feed temperature was fixed at 20°C because it is not the control parameter for the operation. The rate of cross-flow of each solution was adjusted to 0.4, 0.8, and 1.2 L/min to reveal the effect of flow rate. The MD experiments were carried out in the DCMD configuration with the outside-in mode. The temperature of permeate (distillate) solution maintained at 20(±1)°C and feed solutions were adjusted to 40(±1)°C, 50(±1)°C, and 60(±1)°C. The flow rate of the feed solution was controlled to 0.4, 0.8, and 1.2 L/min. The flow rate of the distillate was adjusted from 0.1 to 0.4 L/min. Details on the test conditions are summarized in Table 2.

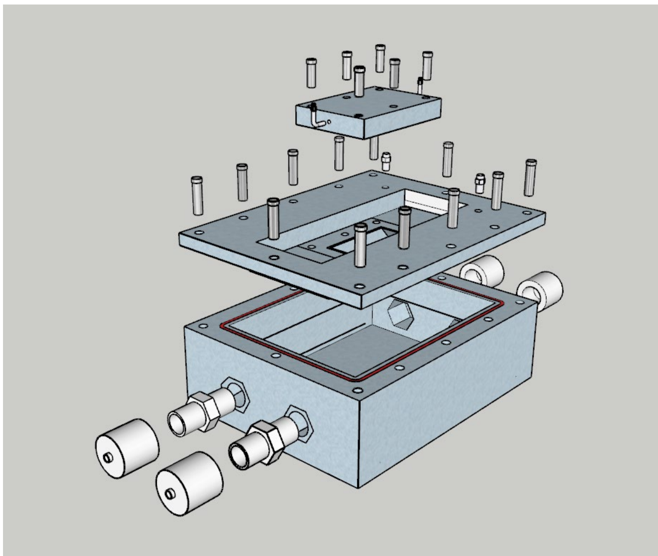

Fig. 2. Circumstantial modular configurations of the integrated FO-MD module.

3. Results and discussion

3.1. Effect of flow rate on FO flux

In the FO-MD hybrid process, it is necessary to have a balance between the FO flux and the MD flux. Otherwise, a steady-state condition cannot be achieved. Accordingly, it is necessary to know the factors affecting the FO flux and MD flux. To begin, the effect of flow rates of the feed and draw solutions on the FO flux was investigated in the integrated FO-MD module. The tests were carried out using 1.0 M NaCl solution as the draw solution. In Fig. 3a, the flow rate of the FO feed solution was adjusted from 0.4 to 1.2 L/min while the flow rate of the draw solution was fixed

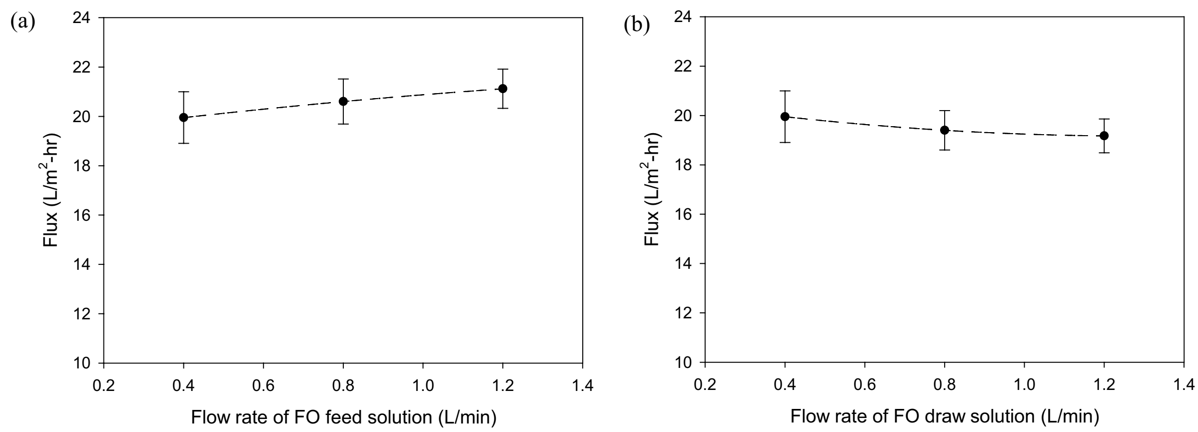

Fig. 3. Effect of flow rate in the FO process in the integrated FO-MD module. (a) Flow rate of feed solution and (b) flow rate of draw solution.

Table 2
Experimental conditions of single module tests

		FO	DCMD
Flow rate (L/min)	FS	0.4, 0.8, 1.2	0.4, 0.8, 1.2
	DS/permeate	0.4, 0.8, 1.2	0.1, 0.4
Temperature (±°C)	FS	20	40, 50, 60
	DS/permeate	40, 50, 60	20

at 0.4 L/min. The temperatures of both solutions were set to 20(±1)°C. As expected, the average water flux increased as an increase in the feed flow rate. In the integrated FO-MD module, the average flux increased from 19.9 to 21.1 L/m^2 h as the feed flow rate increased from 0.4 to 1.2 L/min, which corresponds to about 6% rise. Since an increase in the feed flow rate reduces the external concentration polarization (ECP), the flux can be improved. Nevertheless, the flux was not sensitive to the feed flow rate because the ECP was less important than the ICP in FO processes [41].

In Fig. 3b, the flow rate of the draw solution was changed from 0.4 to 1.2 L/min while the feed flow rate was constant at 0.4 L/min. Again, the temperatures on both sides were fixed at 20(±1)°C. Unlike the previous case, an increase in the flow rate of the draw solution did not result in an increase in FO flux. As a matter of fact, the average flux slightly decreased from 19.9 to 19.2 L/m^2 h by increasing the flow rate of the draw solution from 0.4 to 1.2 L/min. This is attributed to the ICP on the draw solution side in FO processes. Since the ICP occurs inside the porous support of the FO membrane, it is not easily affected by the flow of the draw solution [17]. Instead, an increase in the flow rate of the draw solution may result in an adverse impact by increasing the pressure on the draw side, it may cause a slight reduction in the FO flux. In summary, it appears that the FO flux cannot be easily controlled by adjusting the flow rates of the feed and draw solutions.

3.2. *Effect of flow rate on MD flux*

A set of MD experiments were carried out to examine the effect of the flow rate on MD flux in the integrated FO-MD module. In this case, the feed solution of the MD membrane is the same as the draw solution of the FO membrane. In Fig. 4a, the flow rate of the MD feed solution was adjusted from 0.4 to 1.2 L/min while the flow rate of the distillate solution was fixed at 0.4 L/min. The temperatures of feed and distillate solutions were 50(±1)°C and 20(±1)°C, respectively. As the feed flow rate increased from 0.4 to 1.2 L/min, the MD flux increased from 1.34 to 2.5 L/m^2 h, indicating that the MD flux is sensitive to the feed flow rate. This is because the temperature polarization (TP) in MD can be reduced by increasing the feed flow rate [31]. Since the TP on the feed side is a major factor limiting the MD flux, the reduction of the TP by the increased feed flow rate leads to an increased flux.

In Fig. 4b, the flow rate of the distillate (permeate) solution was adjusted to 0.1 and 0.4 L/min, respectively. Due to the limited cross-sectional area of the flow channel inside the hollow fiber membranes, it was not possible to further increase the flow rate of the distillate solution. Nevertheless, it is evident that the MD flux was affected by the distillate flow rate. The MD flux was 0.96 L/m^2 h at 0.1 L/min and 1.31 L/m^2 h at 0.4 L/min, respectively. Again, this can be explained by the TP effect. Since the TP also occurs on the distillate side, an increase in the distillate flow rate reduces the TP, thereby increasing the MD flux. Based on these results, it can be concluded that the MD flux can be controlled to a certain degree by regulating the flow rates of the feed and distillate solutions.

3.3. *Effect of draw solution (DS) temperature on FO flux*

As the next step, the temperature of the draw solution in FO was changed to examine its effect on the FO flux. It should be mentioned that the FO draw solution is the same as the MD feed solution. Thus, the temperature of the FO draw solution should be higher than that of the FO feed solution. In Fig. 5a, the temperature of the draw solution was set to 40(±1)°C, 50(±1)°C, and 60(±1)°C while the feed temperature was 20(±1)°C. The flow rates of the feed and draw solutions were 0.4 and 0.8 L/min, respectively. Results showed that the temperature of the draw solution did not significantly affect the FO flux. The FO flux was 18.8 L/m^2 h at

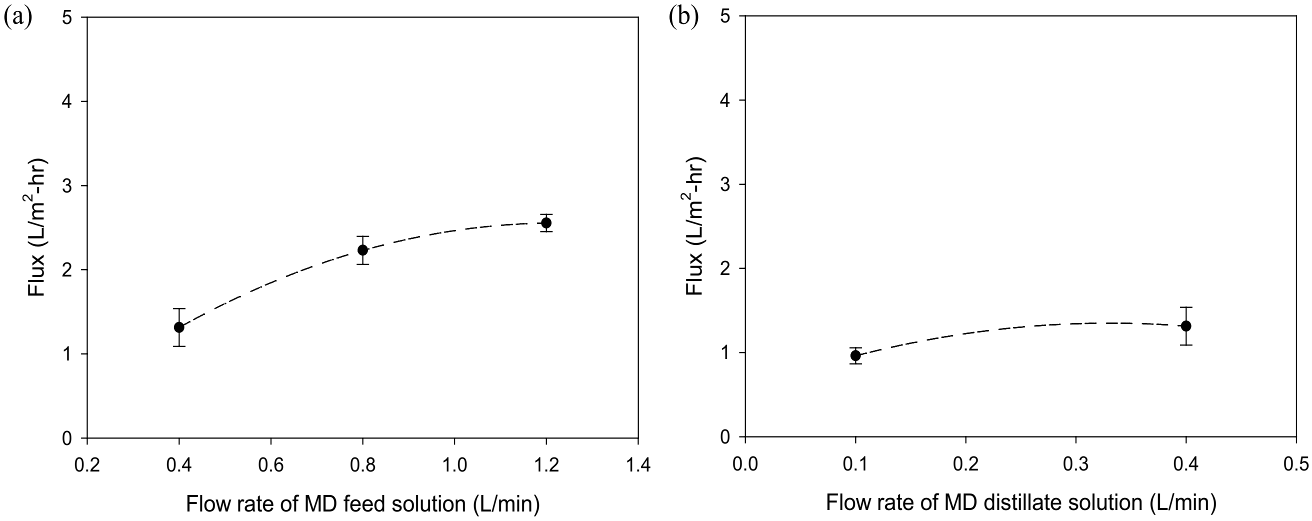

Fig. 4. Effect of flow rate in the hollow-fiber DCMD process in the integrated FO-MD module. (a) Flow rate of feed solution and (b) flow rate of distillate solution.

40(±1)°C and 18.5 L/m^2 h at 60(±1)°C. According to the van't Hoff equation, the osmotic pressure increases with the temperature. However, the effect seems to be negligible between 40°C and 60°C, which corresponds to 0.64% from the theory [42,43]. The water permeability of the FO membrane is affected by the feed temperature rather than the draw solution temperature, suggesting that the FO flux is not sensitive to the temperature on the draw solution side. On the other hand, the FO flux may be slightly reduced by the effect of the thermal-osmosis phenomenon [44,45], which makes the water move from the hot side to cold side. It appears that the thermal-osmosis phenomenon decreased the FO flux with an increase in the draw solution temperature.

3.4. Effect of feed solution (FS) temperature on MD flux

The dependence of the MD flux on the feed temperature in the integrated FO-MD module was shown in Fig. 5b. The flow rate and the temperature of the distillate solution were 0.4 L/min and 20(±1)°C, respectively. The MD flux proportionally increased with the feed solution temperature. The MD flux was 0.7 L/m^2 h at 40(±1)°C and increased up to 3.8 L/m^2 h at 60(±1)°C. This is attributed to an increase in the driving force with the temperature difference between the feed and distillate solutions [31].

3.5. FO-MD hybrid system using separate FO and MD modules

The two-hybrid systems are shown in Fig. 1 was compared. First, the hybrid system consisting of a FO module and an MD module (Fig. 1a) was used to examine the flux behavior in FO and MD. In Fig. 6a, the temperatures of the FO feed, draw solution, and distillate was 20(±1)°C, 50(±1)°C, and 20(±1)°C, respectively. The flow rates of the FO feed, draw solution, and distillate was 0.4, 0.8, and 0.4 L/min, respectively. The initial FO flux was 18.6 L/m^2 h and decreased to 13.0 L/m^2 h with time, which corresponds to a 30% reduction in FO flux. On the other hand, the MD flux was almost constant at 1.68 L/m^2 h. It seems that the amount of water passing through the FO membrane was larger than that that through the MD membrane, leading to a net dilution of the draw solution with time. Although the water balance between FO and MD was set to achieve the steady-state, it did not maintain during the operation of the hybrid system.

Accordingly, the temperature of the MD feed solution (FO draw solution) was increased from 50(±1)°C to 60(±1)°C in the middle of the operation. The results are shown in Fig. 6b. With the increase in the temperature after 600 min, the MD flux increased from 1.8 to 2.71 L/m^2 h. This led to an increase in the FO flux by 9%. Nevertheless, the FO flux began to decrease after 1,400 min, indicating that the stable operation of the FO-MD hybrid system is difficult using the separate modules. Since the constant flux is desired in practical membrane processes, these flux behaviors may be problematic in this FO-MD hybrid system.

3.6. FO-MD hybrid system using an integrated module

In Fig. 7a, the FO and MD fluxes are shown as a function of time in the FO-MD hybrid system using the integrated module. The temperature of the FO draw solution was fixed at 50(±1)°C. The normalized water flux of FO was reduced to 0.8 at the end of the experiment. The MD flux slightly increases with time and its average value was 2.06 L/m^2 h. The normalized water flux of FO was reduced to 0.8 at the end of the experiment. Compared with the results in the hybrid system using two separate modules (Fig. 6a), the FO flux was more stable and the MD flux was higher by approximately 20%.

To obtain more stable FO flux, the temperature of the draw solution was adjusted between 50(±1)°C and 60(±1)°C at 400; 1,200; and 2,800 min. As shown in Fig. 7b, the FO flux was almost constant during the operation of the integrated FO-MD module. The MD flux was controlled between 2.12 and 3.95 L/m^2 h by the temperature, allowing

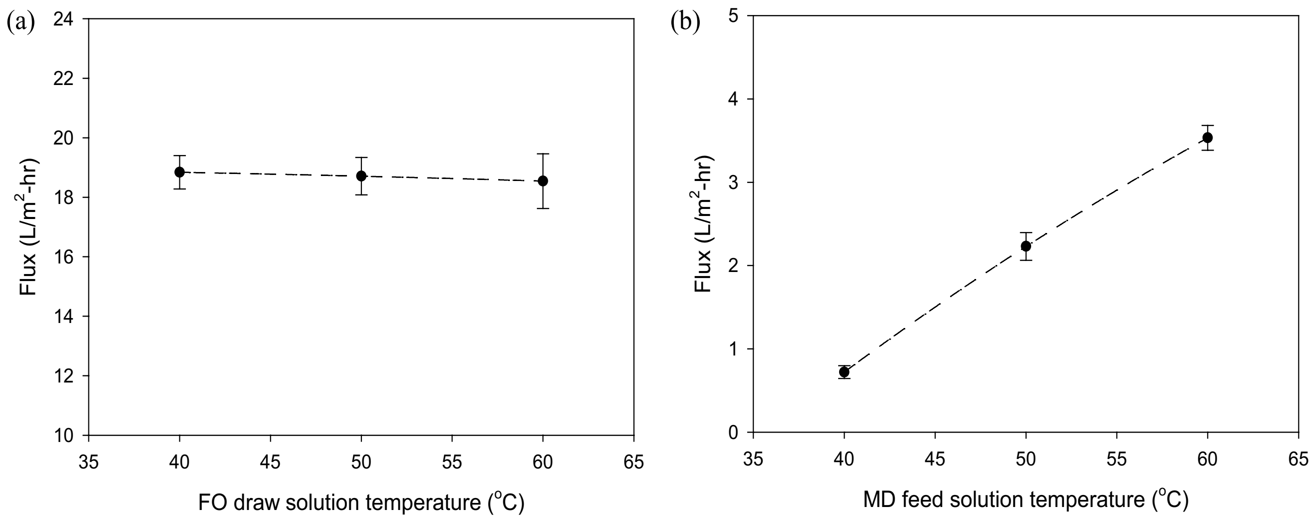

Fig. 5. Effect of solution temperature in the FO process in the integrated FO-MD module. (a) Draw solution temperature and (b) feed solution temperature.

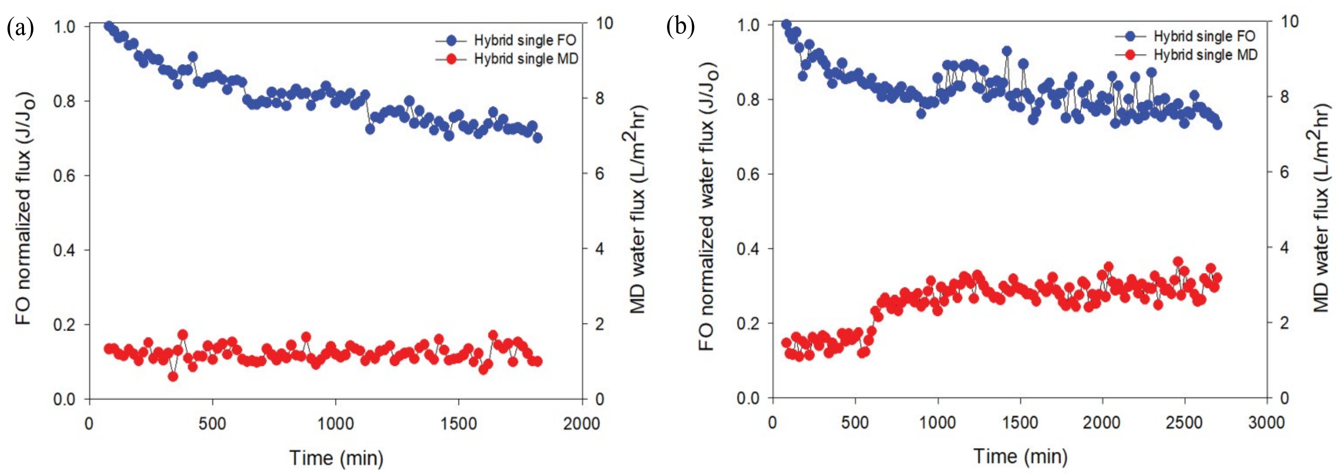

Fig. 6. Flux behaviors in the FO-MD hybrid system using separate FO and MD modules. (a) Constant temperature of the draw solution at 50°C and (b) adjustment of the temperature of the draw solution between 50°C and 60°C.

the adjustment of the concentration of the draw solution. In fact, the conductivity of the draw solution was changed from 80.5 to 83.5 mS/cm, allowing the constant flux operation of FO. Fig. 7c confirms the establishment of the water balance between FO and MD. In summary, it is evident from the results that the constant flux operation of FO can be done by adjusting the draw solution temperature in the FO-MD hybrid system using the integrated module.

The mechanism of the flux control in the integrated module can be explained as follows: when the FO flux is reduced during the operation, an action is taken to increase the temperature of the draw solution. This leads to an increase in the MD flux, thereby raising the concentration of the draw solution. Accordingly, the osmotic pressure of the draw solution increases to raise up the FO flux. If the FO flux is too high, the temperature of the draw solution is reduced to decrease the draw solution concentration. Again, the FO flux can be adjusted by this control action. Thus, the control of the FO flux can be relatively easy with the integrated module in the FO-MD hybrid system.

4. Conclusion

In this study, the effect of operating conditions on the performance of FO-MD hybrid systems was investigated. A novel technique that integrated flat sheet FO and hollow fiber MD membranes into a single module was attempted. As a result of this study, the following conclusions were drawn:

- In the integrated module, the FO flux slightly increased with an increase in the flow rate of the feed solution. Nevertheless, the FO flux was not significantly affected by the flow rate of the draw solution. The average FO flux ranged from 19 to 21.1 L/m^2 h.

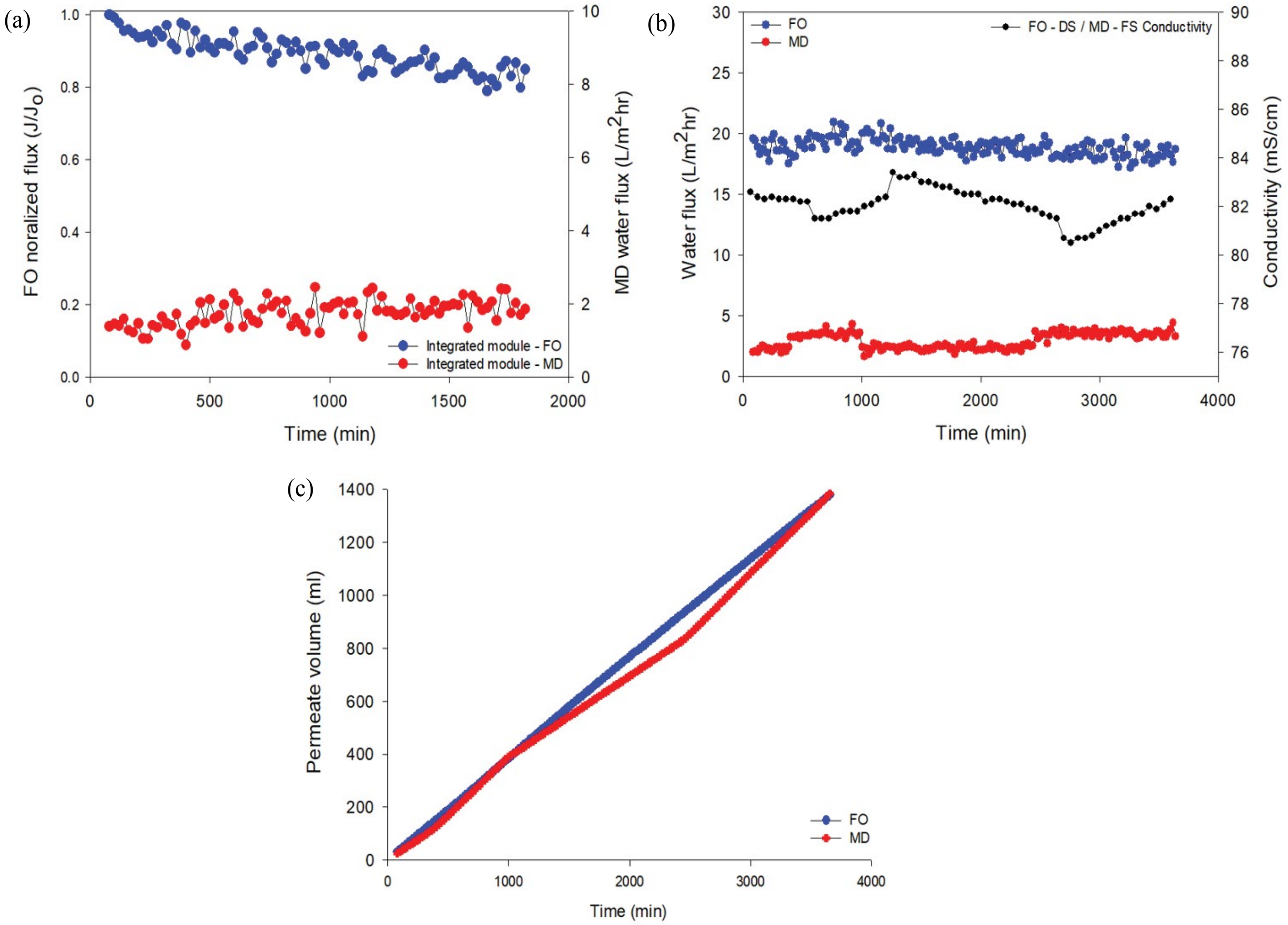

Fig. 7. Flux behaviors in the FO-MD hybrid system using an integrated module. (a) Constant temperature of the draw solution at 50°C, (b) adjustment of the temperature of the draw solution between 50°C and 60°C, and (c) comparison of the permeate volumes from FO and MD membranes.

- The MD flux was sensitive to the flow rate of the feed solution. The average FO flux ranged from 1.34 to 2.5 L/m^2 h. This is because the temperature polarization (TP) in MD can be reduced by increasing the flow rate of the feed solution. The MD flux was also affected by the flow rate of the distillate solution but its influence was less significant.
- The temperature of the draw solution did not significantly affect the FO flux. A slightly decrease in the FO flux was observed with an increase in the temperature. This may be attributed to the effect of the thermal-osmosis phenomenon. On the contrary, the MD flux increased with the temperature of the MD feed solution, which is the same as the FO draw solution in the integrated module. The MD flux was 0.7 L/m^2 h at 40(±1)°C and increased up to 3.8 L/m^2 h at 60(±1)°C.
- In the FO-MD hybrid system using separate FO and MD modules, the FO flux was unstable during the operation. Although the water balance between the FO and MD was set in the beginning, it changed with time, leading to a net reduction in the FO flux.
- In the FO-MD hybrid system using an integrated module, the FO flux was more stable than the hybrid system using the separate modules. Periodic adjustment of the draw solution temperature led to the constant flux operation of the FO process.

Acknowledgment

This work was supported by Korea Environment Industry & Technology Institute (KEITI) through Industrial Facilities & Infrastructure Research Program, funded by Korea Ministry of Environment (MOE) (1485016423)

References

[1] M. Pedro-Monzonís, A. Solera, J. Ferrer, T. Estrela, J. Paredes-Arquiola, A review of water scarcity and drought indexes in water resources planning and management, J. Hydrol., 527 (2015) 482–493.
[2] S.N. Gosling, N.W. Arnell, J.A. Lowe, The implications of climate policy for avoided impacts on water scarcity, Procedia Environ. Sci., 6 (2011) 112–121.
[3] K.J. Lu, Z.L. Cheng, J. Chang, L. Luo, T.-S. Chung, Design of zero liquid discharge desalination (ZLDD) systems consisting of freeze desalination, membrane distillation, and crystallization powered by green energies, Desalination, 458 (2019) 66–75.
[4] V. Belessiotis, S. Kalogirou, E. Delyannis, Thermal Solar Desalination: Methods and Systems, Elsevier, 2016.
[5] N. Misdan, W.J. Lau, A.F. Ismail, Seawater reverse osmosis (SWRO) desalination by thin-film composite membrane—

current development, challenges, and future prospects, Desalination, 287 (2012) 228–237.

[6] S. Kim, D. Cho, M.-S. Lee, B.S. Oh, J.H. Kim, I.S. Kim, SEAHERO R&D program and key strategies for the scale-up of a seawater reverse osmosis (SWRO) system, Desalination, 238 (2009) 1–9.

[7] J. Kim, K. Park, D.R. Yang, S. Hong, A comprehensive review of energy consumption of seawater reverse osmosis desalination plants, Appl. Energy, 254 (2019) 113652.

[8] S. Lee, J. Choi, Y.-G. Park, H. Shon, C.H. Ahn, S.-H. Kim, Hybrid desalination processes for beneficial use of reverse osmosis brine: current status and future prospects, Desalination, 454 (2019) 104–111.

[9] G.U. Semblante, J.Z. Lee, L.Y. Lee, S.L. Ong, H.Y. Ng, Brine pre-treatment technologies for zero liquid discharge systems, Desalination, 441 (2018) 96–111.

[10] H. Frank, K.E. Fussmann, E. Rahav, E. Bar Zeev, Chronic effects of brine discharge form large-scale seawater reverse osmosis desalination facilities on benthic bacteria, Water Res., 151 (2019) 478–487.

[11] B.K. Pramanik, L. Shu, V. Jegatheesan, A review of the management and treatment of brine solutions, Environ. Sci.: Water Res. Technol., 3 (2017) 625–658.

[12] R. Connor, The United Nations World Water Development Report 2015, Vol. 1, Water for a Sustainable World, UNESCO Publishing, 2015.

[13] T. Tong, M. Elimelech, The global rise of zero liquid discharge for wastewater management: drivers, technologies, and future directions, Environ. Sci. Technol., 50 (2016) 6846–6855.

[14] W.L. Ang, A. Wahab Mohammad, D. Johnson, N. Hilal, Forward osmosis research trends in desalination and wastewater treatment: a review of research trends over the past decade, J. Water Process Eng., 31 (2019) 100886.

[15] C. Klaysom, T.Y. Cath, T. Depuydt, I.F. Vankelecom, Forward and pressure retarded osmosis: potential solutions for global challenges in energy and water supply, Chem. Soc. Rev., 42 (2013) 6959–6989.

[16] E.W. Tow, D.M. Warsinger, A.M. Trueworthy, J. Swaminathan, G.P. Thiel, S.M. Zubair, A.S. Myerson, J.H. Lienhard V, Comparison of fouling propensity between reverse osmosis, forward osmosis, and membrane distillation, J. Membr. Sci., 556 (2018) 352–364.

[17] N. Akther, A. Sodiq, A. Giwa, S. Daer, H.A. Arafat, S.W. Hasan, Recent advancements in forward osmosis desalination: a review, Chem. Eng. J., 281 (2015) 502–522.

[18] M. Qasim, N.A. Darwish, S. Sarp, N. Hilal, Water desalination by forward (direct) osmosis phenomenon: a comprehensive review, Desalination, 374 (2015) 47–69.

[19] Y.-N. Wang, K. Goh, X. Li, L. Setiawan, R. Wang, Membranes and processes for forward osmosis-based desalination: recent advances and future prospects, Desalination, 434 (2018) 81–99.

[20] W.A. Suwaileh, D.J. Johnson, S. Sarp, N. Hilal, Advances in forward osmosis membranes: altering the sub-layer structure via recent fabrication and chemical modification approaches, Desalination, 436 (2018) 176–201.

[21] S. Phuntsho, S. Hong, M. Elimelech, H.K. Shon, Forward osmosis desalination of brackish groundwater: meeting water quality requirements for fertigation by integrating nanofiltration, J. Membr. Sci., 436 (2013) 1–15.

[22] J.E. Kim, S. Phuntsho, S.M. Ali, J.Y. Choi, H.K. Shon, Forward osmosis membrane modular configurations for osmotic dilution of seawater by forward osmosis and reverse osmosis hybrid system, Water Res., 128 (2018) 183–192.

[23] B. Al Hawli, A. Benamor, A.A. Hawari, A hybrid electrocoagulation/forward osmosis system for treatment of produced water, Chem. Eng. Process. Process Intensif., 143 (2019) 107621.

[24] World first for zero liquid discharge, Filtr. Sep., 53 (2016) 20–22.

[25] S. Phuntsho, J.E. Kim, M.A.H. Johir, S. Hong, Z. Li, N. Ghaffour, T. Leiknes, H.K. Shon, Fertiliser drawn forward osmosis process: pilot-scale desalination of mine impaired water for fertigation, J. Membr. Sci., 508 (2016) 22–31.

[26] Q. Ge, M. Ling, T.-S. Chung, Draw solutions for forward osmosis processes: developments, challenges, and prospects for the future, J. Membr. Sci., 442 (2013) 225–237.

[27] D.J. Johnson, W.A. Suwaileh, A.W. Mohammed, N. Hilal, Osmotic's potential: an overview of draw solutes for forward osmosis, Desalination, 434 (2018) 100–120.

[28] S.Y. Park, H.-W. Ahn, J.W. Chung, S.-Y. Kwak, Magnetic core-hydrophilic shell nanosphere as stability-enhanced draw solute for forward osmosis (FO) application, Desalination, 397 (2016) 22–29.

[29] T.N. Bitaw, K. Park, D.R. Yang, Optimization on a new hybrid forward osmosis-electrodialysis-reverse osmosis seawater desalination process, Desalination, 398 (2016) 265–281.

[30] Y. Zhou, M. Huang, Q. Deng, T. Cai, Combination and performance of forward osmosis and membrane distillation (FO-MD) for treatment of high salinity landfill leachate, Desalination, 420 (2017) 99–105.

[31] M. Khayet, T. Matsuura, Membrane Distillation: Principles and Applications, Elsevier, 2011.

[32] A. Deshmukh, C. Boo, V. Karanikola, S. Lin, A.P. Straub, T. Tong, D.M. Warsinger, M. Elimelech, Membrane distillation at the water-energy nexus: limits, opportunities, and challenges, Energy Environ. Sci., 11 (2018) 1177–1196.

[33] N. Ghaffour, S. Soukane, J.G. Lee, Y. Kim, A. Alpatova, Membrane distillation hybrids for water production and energy efficiency enhancement: a critical review, Appl. Energy, 254 (2019) 113698.

[34] A. Ali, R.A. Tufa, F. Macedonio, E. Curcio, E. Drioli, Membrane technology in renewable-energy-driven desalination, Renewable Sustainable Energy Rev., 81 (2018) 1–21.

[35] U.K. Kesieme, N. Milne, H. Aral, C.Y. Cheng, M. Duke, Economic analysis of desalination technologies in the context of carbon pricing, and opportunities for membrane distillation, Desalination, 323 (2013) 66–74.

[36] Z. Si, D. Han, Y. Song, J. Chen, L. Luo, R. Li, Experimental investigation on a combined system of vacuum membrane distillation and mechanical vapor recompression, Chem. Eng. Process. Process Intensif., 139 (2019) 172–182.

[37] I. Hitsov, T. Maere, K. De Sitter, C. Dotremont, I. Nopens, Modeling approaches in membrane distillation: a critical review, Sep. Purif. Technol., 142 (2015) 48–64.

[38] M.S. Islam, K. Touati, M.S. Rahaman, Feasibility of a hybrid membrane-based process (MF-FO-MD) for fracking wastewater treatment, Sep. Purif. Technol., 229 (2019) 115802.

[39] W. Suwaileh, D. Johnson, D. Jones, N. Hilal, An integrated fertilizer driven forward osmosis-renewables powered membrane distillation system for brackish water desalination: a combined experimental and theoretical approach, Desalination, 471 (2019) 114126.

[40] T. Husnain, Y. Liu, R. Riffat, B. Mi, Integration of forward osmosis and membrane distillation for sustainable wastewater reuse, Sep. Purif. Technol., 156 (2015) 424–431.

[41] Z. Li, L. Jiang, C. Tang, Investigation on removing recalcitrant toxic organic polluters in coking wastewater by forward osmosis, Chin. J. Chem. Eng., 28 (2020) 122–135.

[42] S. Phuntsho, S. Vigneswaran, J. Kandasamy, S. Hong, S. Lee, H.K. Shon, Influence of temperature and temperature difference in the performance of forward osmosis desalination process, J. Membr. Sci., 415 (2012) 734–744.

[43] A.H. Hawari, N. Kamal, A. Altaee, Combined influence of temperature and flow rate of feeds on the performance of forward osmosis, Desalination, 398 (2016) 98–105.

[44] J. Mengual, F.G. López, C. Fernandez-Pineda, Permeation and thermal osmosis of water through cellulose acetate membranes, J. Membr. Sci., 26 (1986) 211–230.

[45] J. Ortiz-Zárate, F.G. Lopez, J. Mengual, Non-isothermal water transport through membranes, J. Membr. Sci., 56 (1991) 181–194.